VIII International Conference on Fracture Mechanics of Concrete and Concrete Structures
FraMCoS-8
J.G.M. Van Mier, G. Ruiz, C. Andrade, R.C. Yu and X.X. Zhang (Eds)

CONSTITUTIVE MODEL FOR STEEL FIBRE REINFORCED CONCRETE IN TENSION

SEONG-CHEOL LEE [*], JAE-YEOL CHO [†] AND FRANK J. VECCHIO [‡]

[*] KEPCO International Nuclear Graduate School (KINGS)
1456-1 Shinam-ri, Seosaeng-myeon, Ulju-gun, Ulsan, 689-882, South Korea
e-mail: sclee@kings.ac.kr

[†] Department of Civil & Environmental Engineering, Seoul National University
599 Gwanak-ro, Gwanak-gu, Seoul, 151-744, South Korea
e-mail: jycho@snu.ac.kr

[‡] Department of Civil Engineering, University of Toronto
35 St. George Street, Toronto, ON, M5S 1A4, Canada
e-mail: fjv@civ.utoronto.ca

Key words: Fibre Reinforced Concrete, Steel Fibre, Tensile Stress, Crack Width, Bond, Anchorage

Abstract: In order to represent the ductile tensile behaviour of steel fibre reinforced concrete (SFRC), the Diverse Embedment Model (DEM) was recently developed, accounting for both the random distribution of fibres and the pull-out behaviour of fibres. Although the DEM shows good agreement with test results measured from uniaxial tension tests, it entails a double numerical integration which complicates its implementation into computational models and software developed for the analysis of the structural behaviour of SFRC members.
In this paper, the DEM is simplified by eliminating the double numerical integration; thus, the Simplified DEM (SDEM) is derived. In order to simplify the DEM, only fibre slip on the shorter embedded side is taken into the account of the fibre tensile stress at a crack, while coefficients for frictional bond behaviour and mechanical anchorage effect are incorporated to prevent overestimation of the tensile stress attained by fibres due to the neglect of fibre slip on the longer embedded side. The tensile stress-crack width response of SFRC predicted by the SDEM shows good agreement with that obtained from the DEM; hence, the model's accuracy has largely been retained despite the simplification. In comparisons with test results reported in the previous literature, the SDEM is shown to simulate well not only the direct tensile behaviour but also the flexural behaviour of SFRC members. The SDEM can easily be implemented in currently available analysis models and programs so that it can be useful in the modelling of structural behaviour of SFRC members or structures.

1 INTRODUCTION

It is well known that steel fibre reinforced concrete (SFRC) exhibits a ductile post-cracking behaviour due to steel fibres bridging cracks. Many researchers [1-4] investigated the beneficial aspect of SFRC in structural members. However, SFRC is yet to be widely applied as a structural member in actual construction. One of the main reasons for this is that most researches focused on qualitative evaluations for the tensile behaviour of SFRC [5-9], rather than on the development of a rational model which can be easily employed to predict the structural behaviour of SFRC members.

Recently, several research groups

developed constitutive models for the tensile behaviour of SFRC members. Marti et al. [10] developed a simple formula to predict the tensile stress-crack width relationship of SFRC, by assuming that the number of fibres bridging a crack decreases linearly with increasing crack width. Later, an engagement factor to consider the effect of fibre inclination angle on fibre pullout behaviour was introduced by Voo and Foster [11] who developed the Variable Engagement Model (VEM). Leutbecher and Fehling [12] also presented a model that considers the effect of fibres on crack widths in SFRC members with conventional reinforcing bars. Stroeven [13] developed a formulation that considered varying uniform bond stress along a fibre according to the fibre type. However, the appropriateness of these models for SFRC members with end-hooked fibres is questionable because a uniform bond stress along a fibre is assumed.

Recently, Lee et al. [14-15] proposed the Diverse Embedment Model (DEM) evaluating the tensile stresses due to the frictional bond behaviour and the mechanical anchorage effect separately so that the tensile behaviour of SFRC with straight fibres or end-hooked fibres could be accurately predicted. In the DEM, however, a double numerical integration should be undertaken in order to calculate the average tensile stress of steel fibres at a crack. This complicates the implementation of the DEM into various analysis models [16-19] and programs [20-21] useful for the calculation of the structural behaviour of SFRC members with or without conventional reinforcing bars.

In this paper, therefore, a simplified version of the DEM (SDEM) will be derived by eliminating the double numerical integration in the DEM by introducing some coefficients without significant loss of accuracy.

2 DERIVATION OF THE SIMPLIFIED DEM (SDEM)

2.1 Fundamental assumption

In the DEM formulation, with the assumption of a rigid body translation, the pullout behaviour of a single fibre embedded on both sides can be analyzed, then the average tensile stress of fibres at a crack as the following equation.

$$\sigma_{f,cr,avg} = \frac{2}{l_f}\int_0^{l_f/2}\int_0^{\pi/2}\sigma_{f,cr}\sin\theta\, d\theta dl_a \quad (1)$$

where $\sigma_{f,cr}$ is a fibre tensile stress at a crack, which is a function of the fibre orientation angle (θ) and fibre embedment length (l_a). Although the DEM well predicts the tensile behaviour of SFRC, the calculation of the average fibre tensile stress at a crack is complicating because of a double numerical integration due to the compatibility condition that the crack width be equal to the sum of the slips on both sides of a fibre.

In order to simplify the DEM, one more assumption can be made with respect to compatibility; the crack width can be assumed to be the same as the slip on the shorter embedded side while the slip on the longer embedded side is neglected. With this assumption, the iteration procedure required to analyze the pullout behaviour of a single fibre embedded on both sides can be omitted so that the double numerical integration in the DEM can be averted. However, the effect of fibre slip of the longer embedded side on the fibre tensile stress at a crack can be significant in some cases. Hence, in this paper, two coefficients will be introduced within the formulation to compensate for the relaxed compatibility condition. The details follow.

2.2 Frictional bond behaviour

In the case of straight fibres, since it is assumed that the slip of a fibre occurs only on the shorter embedded side, a fibre tensile stress at a crack can be calculated by integrating the frictional bond stress along the shorter embedment part of the fibre. In this paper, a bilinear relationship between the bond stress and slip is employed for the frictional bond behaviour of a fibre, as illustrated in Fig. 1, which considers the effect of fibre inclination angle on the frictional bond behaviour. The frictional bond strength is constant while the

slip at the peak increases with an increase of the fibre inclination angle, as assumed in the DEM based on test results reported by Banthia and Trottier [23]. Note that the slip reported in the figure is the same as the crack width because the slip of a fibre on the longer embedded side is neglected.

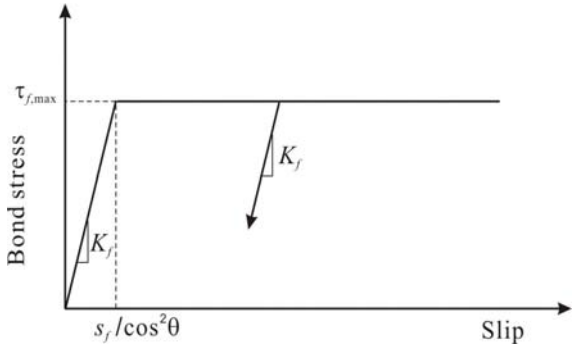

Figure 1: Frictional bond behaviour of a single fibre [22].

Since a bilinear relationship is employed for the frictional bond behaviour, two phases should be considered in the calculation of the fibre tensile stress at a crack. The first occurs when the crack width is so small that all fibres are still on the linearly ascending part of the constitutive law for the frictional bond behaviour; the second prevails when the crack width is large such that some fibres exhibit plastic frictional bond behaviour while other fibres remain in the pre-peak regime.

Without suitable compensation made, the fibre tensile stress can be significantly overestimated when the fibre slip on the longer embedded side is neglected, particularly for a fibre which does not reach the frictional bond strength. This effect of a fibre slip on the longer embedded side quickly diminishes after a fibre reaches the frictional bond strength, because the slip on the longer embedded side decreases as the fibre tensile stress decreases with an increase in the crack width. Therefore, in order to consider the effect of slip of the fibre on the longer embedded side on the frictional bond stress of a fibre, a factor, β_f, will be applied to fibres not having reached the frictional bond strength when the average frictional bond stress or the average fibre tensile stress is calculated.

For the first phase of response in which the crack width is smaller than the slip s_f corresponding to the initiation of plastic frictional bond behaviour of a fibre perpendicular to the crack surface, the average frictional bond stress considering the random distribution of the fibre inclination angle can be calculated as follows:

$$\tau_{f,avg} = \frac{\beta_f}{3}\frac{w_{cr}}{s_f}\tau_{f,\max} \quad \text{for } w_{cr} < s_f \tag{2}$$

where β_f is a coefficient reflecting the effect of fibre slip on the longer embedded side. From comparisons between the average fibre tensile stresses calculated by the DEM and the simplified procedure, it has been analytically determined that β_f is 0.67.

For the second phase of response, in the same manner as for the first phase, the average frictional bond stress considering the random distribution of fibre inclination angle can be derived for the second phase as follows:

$$\tau_{f,avg} = \left(1 - \sqrt{\frac{s_f}{w_{cr}}} + \frac{\beta_f}{3}\sqrt{\frac{s_f}{w_{cr}}}\right)\tau_{f,\max} \quad \text{for } w_{cr} \geq s_f \tag{3}$$

Assuming that the probability density for the shorter embedment length of a fibre is uniform at initial cracking, the average fibre tensile stress at a crack due to the frictional bond behaviour can be calculated as follows:

$$\sigma_{f,cr,st} = \tau_{f,avg}\frac{l_f}{d_f}\left(1 - \frac{2w_{cr}}{l_f}\right)^2 \tag{4}$$

Since the number of fibres bridging a crack surface per unit area is $\alpha_f V_f / A_f$ [24], the tensile stress of SFRC due to the frictional bond behaviour can be calculated as:

$$f_{st} = \alpha_f V_f K_{st}\tau_{f,\max}\frac{l_f}{d_f}\left(1 - \frac{2w_{cr}}{l_f}\right)^2 \tag{5}$$

$$K_{st} = \begin{cases} \dfrac{\beta_f}{3}\dfrac{w_{cr}}{s_f} & \text{for } w_{cr} < s_f \\ 1-\sqrt{\dfrac{s_f}{w_{cr}}}+\dfrac{\beta_f}{3}\sqrt{\dfrac{s_f}{w_{cr}}} & \text{for } w_{cr} \geq s_f \end{cases} \quad (6)$$

In Eq. (5), α_f can be assumed to be 0.5 for a three-dimensional infinite element.

In Fig. 2, the tensile stresses attained by straight fibers as calculated by the SDEM according to Eq. (5), are compared with those predicted by the DEM. It can be seen that tensile stresses calculated by the simplified model show good agreement with those determined with from the more rigorous DEM regardless of the variation of s_f.

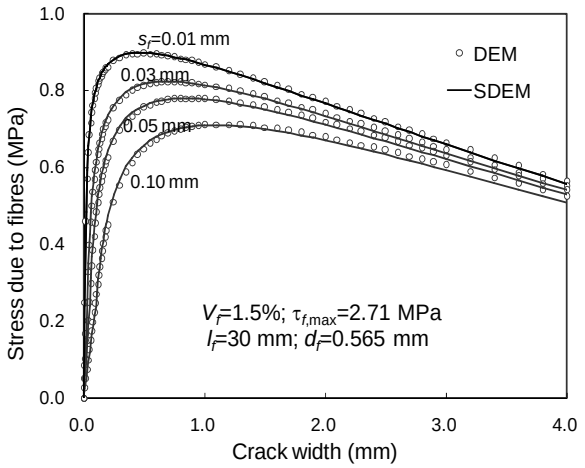

Figure 2: Comparison of SDEM with DEM for straight fibres.

2.3 Mechanical anchorage effect

In the case of end-hooked fibres, the effect of mechanical anchorage on the pullout behaviour should be considered in addition to the frictional bond behaviour. From the test results presented by Banthia and Trottier [23], the effect of fibre inclination angle on the mechanical anchorage effect can be assumed to be the same as for straight fibres; the maximum force due to the mechanical anchorage is constant while the slip at the peak increases with an increase in the fibre inclination angle. Based on the work of Sujivorakul et al. [25], the relationship between fibre slip and tensile force due to the mechanical anchorage is idealized with parabolic and linear relationships for the pre- and post- peak behaviours, respectively, with consideration of the fibre inclination angle effect as illustrated in Fig. 3 [14].

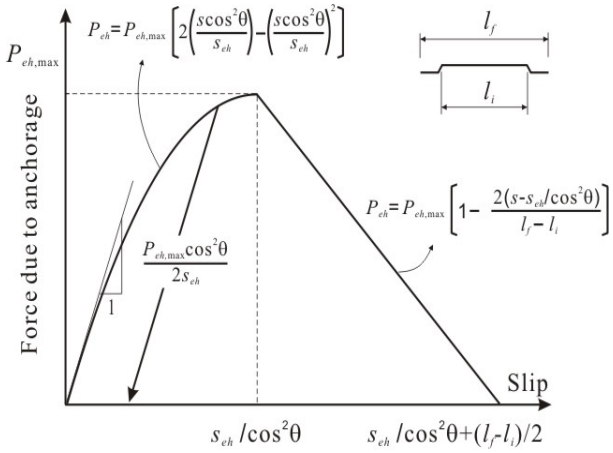

Figure 3: Mechanical anchorage behaviour in an end-hooked fibre [14].

Similar to the frictional bond behaviour, three phases can be considered in the calculation of the fibre tensile stress due to mechanical anchorage; pre-peak, post-peak, and full deterioration of an end-hook. Before the beginning of the full deterioration of an end-hook, through the same procedure presented for the frictional bond behaviour, the average tensile force due to mechanical anchorage can be calculated with consideration given to the random distribution of the fibre inclination angle as follows:

$$P_{eh,avg} = \beta_{eh}\left[\frac{2}{3}\frac{w_{cr}}{s_{eh}}-\frac{1}{5}\left(\frac{w_{cr}}{s_{eh}}\right)^2\right]P_{eh,\max}$$

$$\text{for } w_{cr} < s_{eh} \quad (7)$$

$$P_{eh,avg} = \left[1+\left(\frac{7\beta_{eh}}{15}-1\right)\sqrt{\frac{s_{eh}}{w_{cr}}} - \frac{2\left(\sqrt{w_{cr}}-\sqrt{s_{eh}}\right)^2}{l_f-l_i}\right]P_{eh,\max}$$

$$\text{for } s_{eh} \leq w_{cr} \leq \frac{l_f-l_i}{2} \quad (8)$$

When the crack width is sufficiently large to cause some of end-hooks to fully deteriorate, the equation to evaluate the average tensile force due to mechanical anchorage becomes too difficult to derive exactly through integration. Therefore, a simple parabolic relationship between the crack width and the average tensile force caused by mechanical anchorage can be employed as follows:

$$P_{eh,avg} = \left(\frac{l_i - 2w_{cr}}{2l_i - l_f} \right)^2 P_{eh,avg,i}$$

$$\text{for } \frac{l_f - l_i}{2} \le w_{cr} < \frac{l_i}{2} \qquad (9)$$

where $P_{eh,avg,i}$ is the average tensile force due to the mechanical anchorage at $w_{cr} = \left(l_f - l_i\right)/2$ calculated from Eq. (8).

When the crack width is larger than $l_i/2$, it can be assumed that all mechanical anchorages have fully pulled out.

In the calculation of the average fibre tensile stress at a crack due to the mechanical anchorage effect, the fibres in which the mechanical anchorage has pulled out should not be considered. Therefore, assuming a uniform distribution over the shorter embedment length of fibres at initial cracking, the fibre tensile stress at a crack due to the mechanical anchorage effect can be calculated as follows:

$$\sigma_{f,cr,eh} = \frac{4P_{eh,avg}}{\pi d_f^2} \frac{l_i - 2w_{cr}}{l_f} \qquad (10)$$

By introducing the maximum bond strength due to the mechanical anchorage of an end hooked fibre $\tau_{eh,\max} = 2P_{eh,\max}/\pi d_f l_f$, the tensile stress of an SFRC element due to the mechanical anchorage effect can be calculated as follows:

$$f_{eh} = \alpha_f V_f K_{eh} \tau_{eh,\max} \frac{2\left(l_i - 2w_{cr}\right)}{d_f} \qquad (11)$$

where K_{eh} is referred to Eqs. (7)~(9).

Finally, the tensile stress attained in SFRC elements with end-hooked fibres can be calculated from the superposition of the tensile stresses due to the frictional bond behaviour and the mechanical anchorage effect. Fig. 4 compares the tensile stress attained by end-hooked fibres as calculated by DEM and SDEM. It can be seen that the results of the simplified model show good correspondence with the DEM.

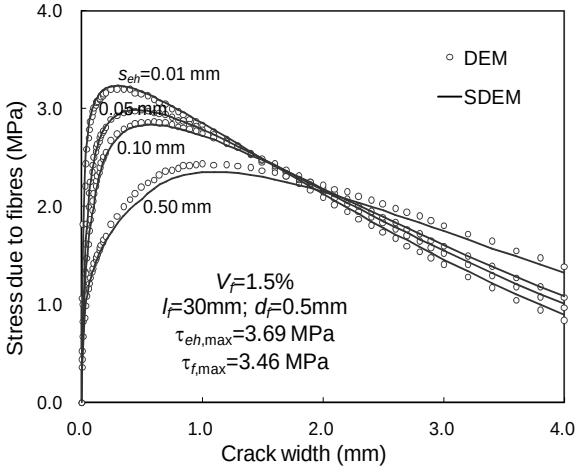

Figure 4: Comparison of SDEM with DEM for end-hooked fibres.

2.4 Tensile stress of SFRC

The formulations above have dealt with the tensile stress attained by steel fibres. To evaluate realistically the tensile stress response of SFRC members, the tensile stress due to the tension softening effect of concrete matrix should be added to that attained by steel fibres. This study adopted the following exponential form [11] for the tension softening effect.

$$f_{ct} = f_{cr} e^{-cw_{cr}} \qquad (12)$$

where the coefficient c is 15 and 30 for concrete and mortar, respectively.

Therefore, the tensile stress of a SFRC member can be calculated as follows:

$$f_{SFRC} = f_f + f_{ct} \qquad (13)$$

where f_f is the tensile stress attained by fibres, equal to f_{st} for straight fibres and $f_{st} + f_{eh}$ for end-hooked fibres.

3 VERIFICATION OF SDEM

3.1 Uniaxial tensile behaviour of SFRC

For the verification of the proposed model, the predictions of SDEM were compared with experimental data obtained from other researchers' investigations [5,26]. The test results were also compared with the predictions of other researchers' proposed models [10-13]. When the SDEM was employed to evaluate the tensile stress attained by steel fibres, the slips corresponding to the bond strength due to the frictional bond behaviour, s_f, and the maximum force due to the mechanical anchorage, s_{eh}, were assumed to 0.01 and 0.1 mm, respectively, as suggested by Naaman and Najm [27]. The frictional bond strength, $\tau_{f,\max}$, and the mechanical anchorage strength, $\tau_{eh,\max}$, were assumed to be $0.396\sqrt{f_c'}$ and $0.429\sqrt{f_c'}$, respectively, based on the previous studies [11,15].

As compared in Fig. 5~6, the SDEM shows the best agreement with the test results not only for the specimens with straight fibres but also for the specimens with end-hooked fibres. This is primarily due to differences in the fundamental assumptions; the SDEM considers both the frictional bond behaviour and the mechanical anchorage effect separately, whereas the other models assumes constant bond stress along fibres even for end-hooked fibres. Therefore, it can be concluded that the structural behaviour of SFRC members subjected to direct tension can be accurately represented by the SDEM.

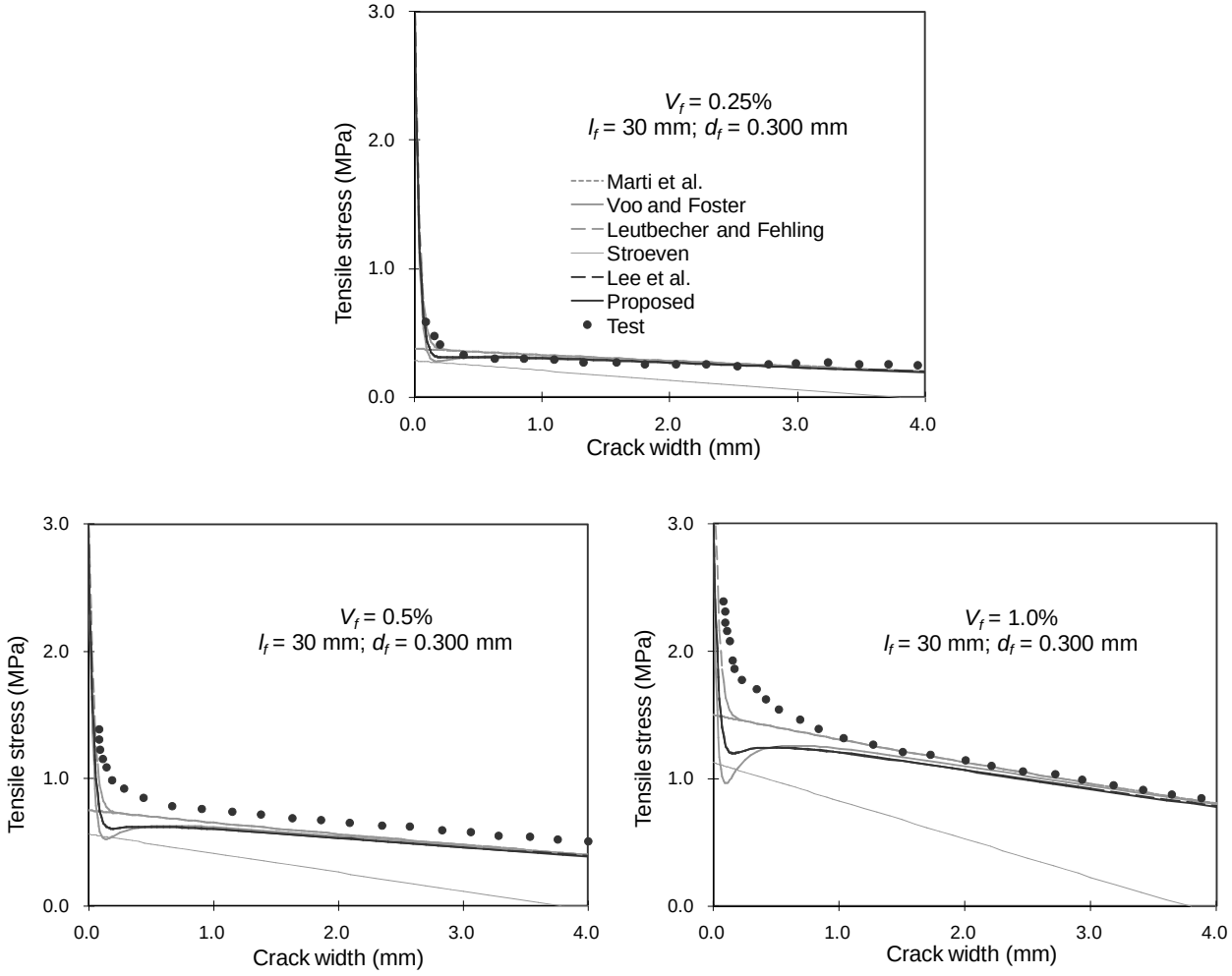

Figure 5: Comparison for the members with straight fibres tested by Petersson [5].

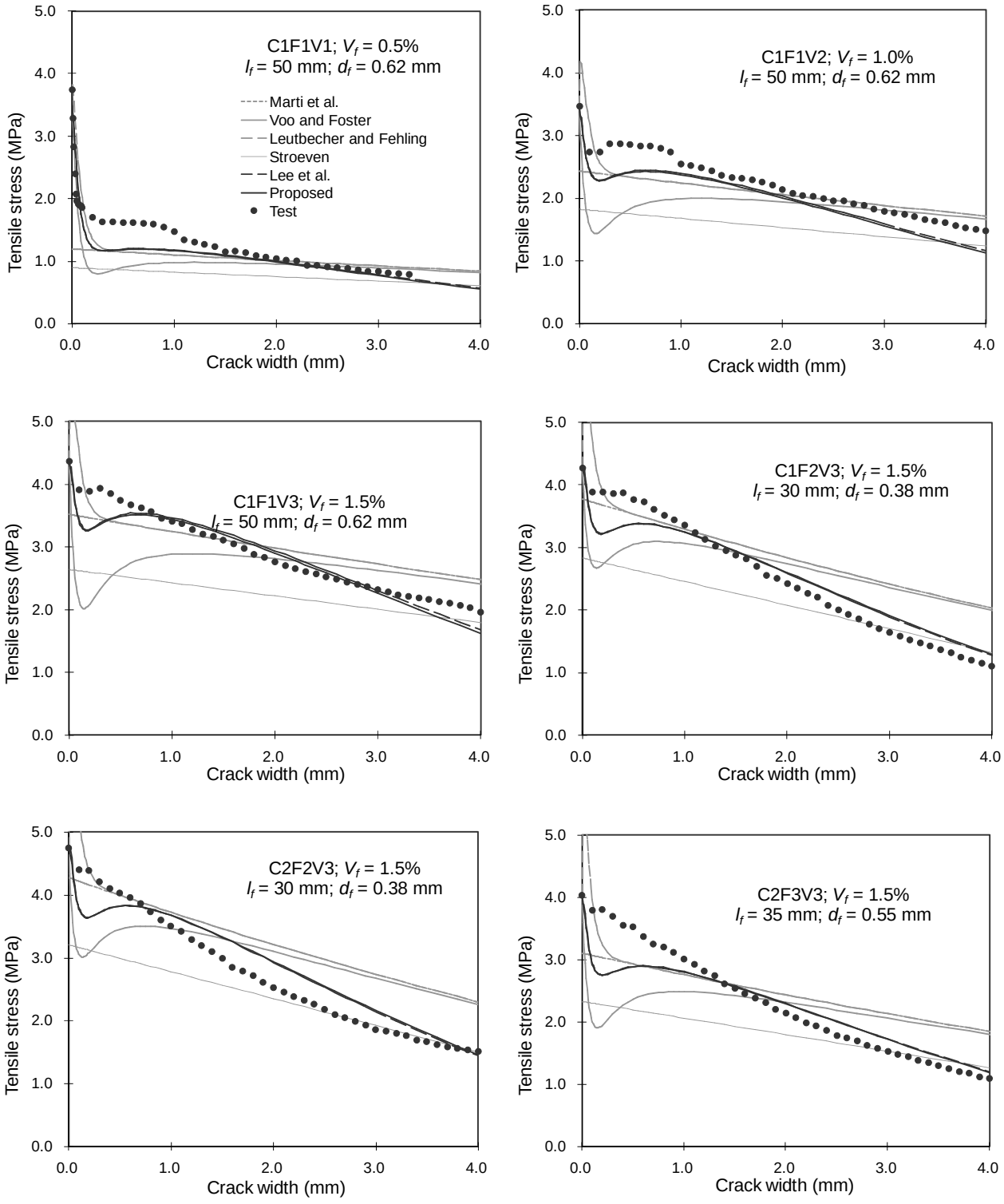

Figure 6: Comparison for the members with end-hooked fibres tested by Susetyo [26].

3.2 Flexural behaviour of SFRC

To investigate the modelling capabilities of the SDEM for flexural members, the four-point bending tests were considered. In the analysis of the flexural behaviour of SFRC specimens, the sectional analysis procedure presented by Oh et al. [28] was employed.

In the flexural analysis, it was assumed that a SFRC beam specimen subjected to the

four-point loading reaches failure through the formation of a single dominant flexural crack, as presented in Fig. 7. From the geometric condition illustrated in this figure, the relationship between the compressive strain of the top fibre in the pure bending region and the centre deflection can be derived. Then, as illustrated in Fig. 8, the stress distribution along the section with a flexural crack can be separately evaluated for the un-cracked depth with the strain distribution and the cracked depth with the crack width distribution. Consequently, the sectional analysis for a section with a flexural crack can be conducted.

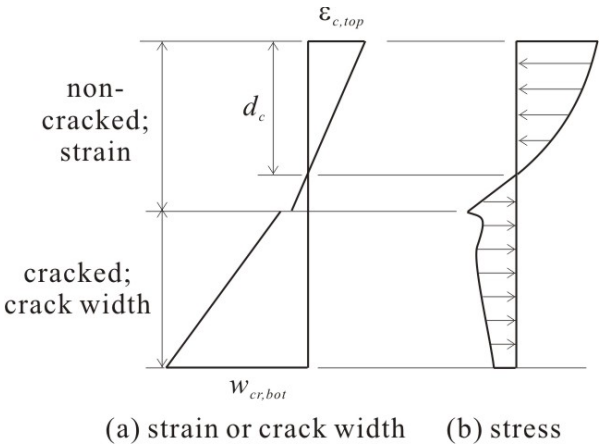

Figure 8: Strain and stress distribution through the section with a crack.

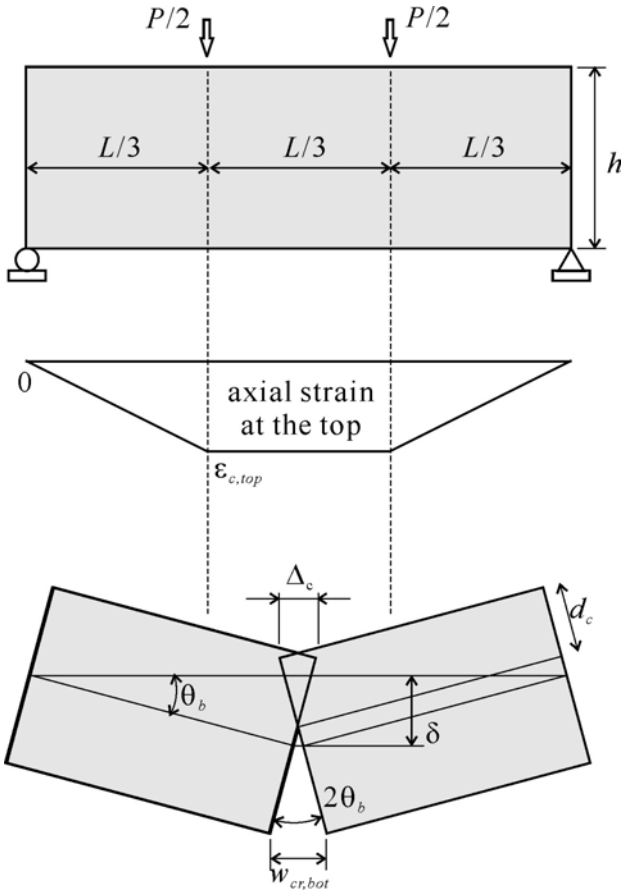

Figure 7: Failure model of a SFRC beam with a single dominant crack [28].

As a verification of the SDEM, the flexural specimens tested by Susetyo [26] were analyzed. As shown in Fig. 9, the analysis results obtained from the SDEM show good agreement with the test results for the flexural behaviour of the SFRC members.

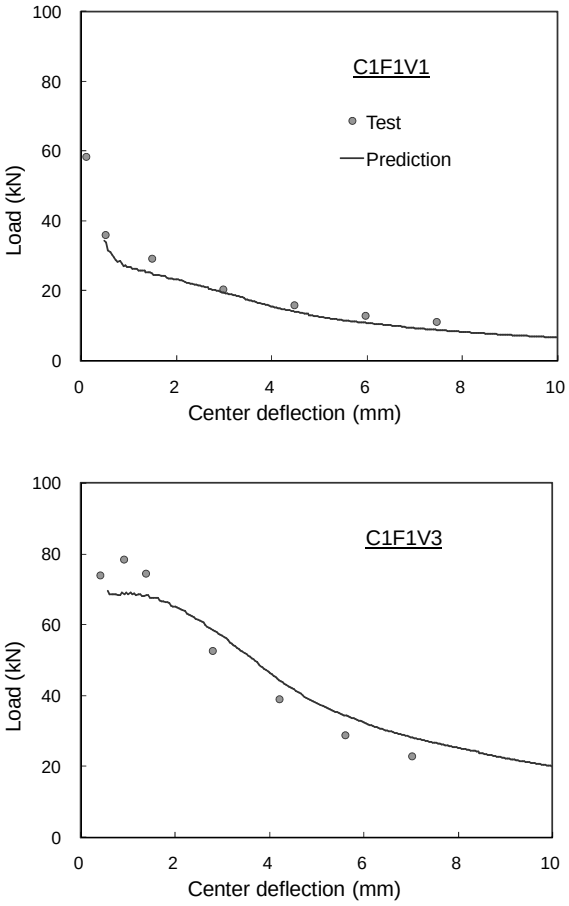

Figure 9: Prediction of the SDEM for the flexural behaviour of SFRC beams tested by Susetyo [26].

4 CONCLUSIONS

In this paper, a simplified version of the Diverse Embedment Model (DEM) was developed by eliminating the double numerical integration procedure. To enable

the simplification, it was assumed that the fibre slip on the shorter embedded side is the same as the crack width. As a result, the fibre tensile stress at a crack can be calculated directly for a given crack width by considering the same constitutive models for frictional bond behaviour and the mechanical anchorage effect as employed in the DEM. To prevent an overestimation of the fibre tensile stress caused by neglecting the effect of a fibre slip on the longer embedded side, the coefficients, β_f and β_{eh} were introduced for the frictional bond behaviour and the mechanical anchorage effect, respectively. Consequently, the tensile stress attained by fibres in SFRC members can be more simply evaluated.

The accuracy of the SDEM was verified through the analysis of various test specimens. The tensile stress-crack width responses of SFRC calculated by the SDEM showed good agreement with those obtained from the DEM. In comparisons with test results, the SDEM predicted well the direct tensile behaviour of SFRC members with straight fibres or end-hooked fibres. From sectional analyses with the failure mode exhibiting a single dominant flexural crack, the SDEM showed also good agreement with the test results for the flexural behaviour of SFRC beams. Consequently, it can be concluded that the tensile or flexural behaviour of SFRC members can be modelled simply and accurately with the SDEM.

The proposed SDEM can be easily implemented into currently available analysis models [19-22] or programs [23-24] so that it can be useful in the assessment of the structural behaviour of SFRC members or structures with or without conventional reinforcing bars.

ACKNOWLEDGEMENT

This research was partially supported by “Basic Science Research Program through the National Research Foundation of Korea (NRF) (20120003756)” funded by the Ministry of Education, Science and Technology.

REFERENCES

[1] Parra-Montesinos, G.J., 2005. High-Performance Fiber-Reinforced Cement Composites: An Alternative for Seismic Design of Structures. *ACI Struct. J.* **102-5**:668-675.

[2] Minelli, F. and Vechcio, F.J., 2006. Compression Field Modeling of Fiber-Reinforced Concrete Members Under Shear Loading. *ACI Struct. J.* **103-2**:244-252.

[3] Dinh, H.H., Parra-Montesinos, G.J. and Wight J.K., 2010. Shear Behavior of Steel Fiber-Reinforced Concrete Beams without Stirrup Reinforcement. *ACI Struct. J.* **107-5**:597-606.

[4] Susetyo, J., Gauvreau, P. and Vecchio, F.J., 2011. Effectiveness of Steel Fiber as Minimum Shear Reinforcement. *ACI Struct. J.* **108-4**:488-496.

[5] Petersson, P.E., 1980. Fracture Mechanical Calculations and Tests for Fiber-Reinforced Concrete in Tension. *Proc. of Adv. in Cem.-Matrix Comp., Mat. Res. Soc.* Boston, 1980; pp. 95-106.

[6] Lim, T.Y., Paramasivam, P. and Lee, S.L., 1987. Analytical Model for Tensile Behavior of Steel-Fiber Concrete. *ACI Mat. J.* **84-4**:286-298.

[7] Li, Z., Li, F., Chang, T.-Y.P. and Mai, Y.-W., 1998. Uniaxial Tensile Behavior of Concrete Reinforced with Randomly Distributed Short Fibers. *ACI Mat. J.* **95-5**:564-574.

[8] Groth, P., 2000. Fibre Reinforced Concrete – Fracture Mechanics Methods Applied on Self-Compacting Concrete and Energetically Modified Binders. Doctoral Thesis, Department of Civil and Mining Engineering, Division of Structural Engineering, Luleå University of Technology, Sweden, 237.

[9] Barragán, B.E., Gettu, R., Martín, M.A. and Zerbino, R.L. 2003. Uniaxial Tension Test for Steel Fibre Reinforced Concrete – A Parametric Study. *Cem. Conc. Comp.* **25-7**:767-777.

[10] Marti, P., Pfyl, T., Sigrist V. and Ulaga T., 1999. Harmonized Test Procedures

for Steel Fiber-Reinforced Concrete. *ACI Mat. J.* **96-6**:676-686.

[11] Voo, J.Y.L. and Foster, S.J., 2003. Variable Engagement Model for Fibre Reinforced Concrete in Tension. *Uniciv Report No. R-420, School of Civil and Environmental Engineering, The University of New South Wales*, June 2003, 86 pp.

[12] Leutbecher, T. and Fehling E., 2008. Crack Width Control for Combined Reinforcement of Rebars and Fibers Exemplified by Ultra-High-Performance Concrete. *fib Task Group 8.6, Ultra High Performance Fiber Reinforced Concrete – UHPFRC*, September 2008; pp. 1-28.

[13] Stroeven, P., 2009. Stereological Principles of Spatial Modeling Applied to Steel Fiber-Reinforced Concrete in Tension. *ACI Mat. J.* **106-3**: 213-222.

[14] Lee, S.-C., Cho, J.-Y. and Vecchio, F.J., 2011. Diverse Embedment Model for Fiber Reinforced Concrete in Tension: Model Development. *ACI Mat. J.* **108-5**:516-525.

[15] Lee, S.-C., Cho, J.-Y. and Vecchio, F.J., 2011. Diverse Embedment Model for Fiber Reinforced Concrete in Tension: Model Verification. *ACI Mat. J.* **108-5**:526-535.

[16] Vecchio, F.J. and Collins, M.P., 1986. The Modified Compression Field Theory for Reinforced Concrete Elements Subjected to Shear. *ACI J.* **83-2**:219-231.

[17] Vecchio, F.J., 2000. Disturbed Stress Field Model for Reinforced Concrete: Formulation. *J. Struc. Eng., ASCE* **126-9**:1070-1077.

[18] Vecchio, F.J., 2001. Disturbed Stress Field Model for Reinforced Concrete: Implementation. *J. Struc. Eng., ASCE* **127-1**:12-20.

[19] Lee, S.-C., Cho, J.-Y. and Vecchio, F.J., 2012. Tension Stiffening Model for Steel Fiber Reinforced Concrete Containing Conventional Reinforcement. *ACI Struc. J.* accepted.

[20] Bentz, E.C., 2000. Sectional Analysis of Reinforced Concrete Members. *Doctorate Thesis, Department of Civil Engineering, University of Toronto*, Toronto, ON, Canada, 2000; 184 pp.

[21] Wong, P.S. and Vecchio, F.J., 2002. VecTor2 & FormWorks User's Manual. *Publication No. 2002-02, Department of Civil Engineering, University of Toronto*, Toronto, ON, Canada, August 2002; 214 pp.

[22] Nammur, Jr.G. and Naaman, A.E., 1989. Bond Stress Model for Fiber Reinforced Concrete Based on Bond Stress-Slip Relationship. *ACI Mat. J.* **86-1**:45-57.

[23] Banthia, N. and Trottier, J.-F., 1994. Concrete Reinforced with Deformed Steel Fibers, Part I: Bond-Slip Mechanisms. *ACI Mat. J.* **91-5**:320-348.

[24] Soroushian, P., and Lee, C.-D., 1990. Distribution and Orientation of Fibers in Steel Fiber Reinforced Concrete. *ACI Mat. J.* **87-5**:433-439.

[25] Sujivorakul, C., Waas, A.M. and Naaman, A.E., 2000. Pullout Response of a Smooth Fiber with an End Anchorage. *J. Eng. Mech., ASCE* **126-9**:986-993.

[26] Susetyo, J., 2009. Fibre Reinforcement for Shrinkage Crack Control in Prestressed, Precast Segmental Bridges. *Doctorate thesis, the Department of Civil Engineering at the University of Toronto*, Toronto, ON, Canada, 2009; 307 pp.

[27] Naaman, A.E. and Najm, H.,1991. Bond-Slip Mechanisms of Steel Fibers in Concrete. *ACI Mat. J.* 88-2:135-145.

[28] Oh, B.H., Park, D.G., Kim, J.C. and Choi, Y.C., 2005. Experimental and Theoretical Investigation on the Postcracking Inelastic Behavior of Synthetic Fiber Reinforced Concrete Beams. *Cem. Conc. Res.* **35-2**:384-392.